PROCEEDINGS, 44th Workshop on Geothermal Reservoir Engineering
Stanford University, Stanford, California, February 11-13, 2019
SGP-TR-214

Grid Adaptive Harmonic Adsorption Recuperative Power and Cooling System

J.J. Jenks*, Bernard P. McGrail, Paul Porter[a], Radha Motkuri, Nate Phillips

*Pacific Northwest National Laboratory, PO Box 466, Hines, OR 97738
[a]Radmax Technologies 7520 N. Market Street Suite 10 Spokane, WA 99217
*jeromy.jenks@pnnl.gov

Keywords: adsorption, MOF, thermal compressor, geothermal, solar, CCHP

ABSTRACT

We introduce a new non-condensing thermodynamic cycle that uses the chemical adsorption affinity of new nanostructured porous materials in a thermal compressor that eliminates the evaporator, condenser, and high pressure pump in the standard ORC to produce 40% more power from the same temperature heat source and can switch modes to cooling if required. This CCHP system is driven by low-grade heat (T<150 oC) and can operate in ambient temperatures over 40 ºC. There is great interest in extracting economic benefit from the vast quantity of low and mid-grade heat rejected to the environment from primary energy conversion sources. In the U.S., this amounts to approximately 59 quads of wasted thermal energy. Geothermal resources at temperatures between 100 and 200 °C represent an additional very large (100 GWth) and widely geographically dispersed resource. Solar PV panels convert the majority of the incident solar radiation to heat as well. The principal reason why these thermal resources are not more fully exploited is cost. Low grade heat sources have modest exergy that can be turned into useful work. This means that standard power generation equipment, heat exchangers, expanders, pumps, etc. are significantly larger for the amount of power generated and efficiency of standard thermodynamic cycles such as the Rankine cycle are inherently low, less than 10% typically. The resulting high capital and operating costs relative to the amount of revenue that can be generated from power sales is rarely very economically attractive, especially today with low costs for natural gas. Hence there is a pressing need for new concepts that can dramatically bend the cost curve of power production from low grade heat sources. In this presentation, we describe a new non-condensing thermal compression cycle that offers potential for transformational improvements in cost and efficiency as compared with standard ORC systems. Although the thermal compressor described herein can be used for cooling, the focus here will be power generation.

1. INTRODUCTION

There is great interest in extracting economic benefit from the vast quantity of low and mid-grade heat rejected to the environment from primary energy conversion sources. In this U.S., this amounts to approximately 59 quads of wasted thermal energy. Geothermal resources at temperatures between 100 and 200°C represent an additional very large (100 GW_{th}) and widely geographically dispersed resource. If even a small fraction of the geo-pressured and co-produced resource fluids could be used to provide power, economically, it could easily quadruple the United States geothermal energy production output.

The principal reason why these thermal resources are not more fully exploited is cost. Low grade heat sources have modest exergy that can be turned into useful work. This means that standard power generation equipment, heat exchangers, expanders, pumps, etc. are significantly larger for the amount of power generated and efficiency of standard thermodynamic cycles such as the Rankine cycle are inherently low, less than 10% typically. The resulting high capital and operating costs relative to the amount of revenue that can be generated from power sales is rarely very economically attractive, especially today with low costs for natural gas. Hence there is a pressing need for new concepts that can dramatically bend the cost curve of power production from low grade heat sources.

In this paper, we describe a new non-condensing thermal compression cycle that offers potential for transformational improvements in cost and efficiency as compared with standard ORC systems.

2. Harmonic Adsorption Recuperative Power (HARP) Cycle

Figure 1 provides a schematic of a standard ORC system configuration. Using R134a as a working fluid, we can set the state points across the ORC expander to be an inlet pressure and temperature of 30 bar and 86°C and outlet conditions of 9 bar and 37°C. Assuming an ambient temperature of cooling water or air at the condenser of 30°C, the vapor is condensed and the latent heat of condensation rejected to the environment. After exiting the condenser, a pump then raises the liquid refrigerant pressure to approximately 30 bar for input to the evaporator where heat is added and the refrigerant vaporized. Using the NIST thermochemical database for R134a and an assumed working fluid flow rate of 0.65 kg/s for this example, these state points give a maximum power output for the cycle of approximately 5.2 kW and heat dissipation to the environment of approximately 120 kW_{th}. As is apparent from these numbers, overall cycle efficiency is low (≈4.6%) and the evaporator/condensing units are quite large due to the large excess heat injection/rejection required and inefficient heat transfer in the vapor phase sections of these components. Furthermore, as ambient temperature rises above the case assumed here of 30°C, less heat can be rejected from the condenser raising the temperature and back pressure on the ORC engine, which reduces power output from the cycle. At high enough ambient temperature, condensation of R134a cannot be achieved and the ORC system cannot generate power.

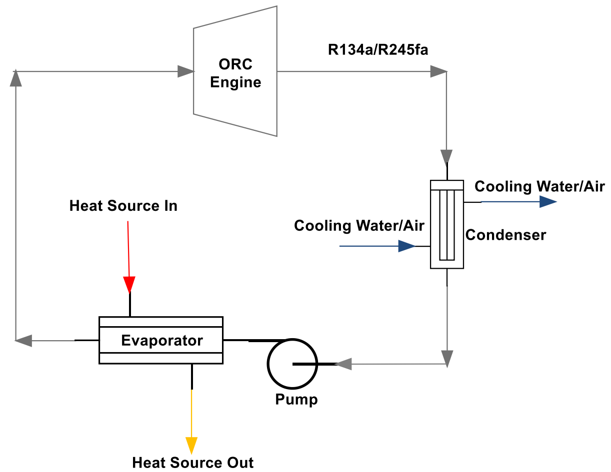

Figure 1. Schematic of Standard ORC System

Figure 2 shows a schematic of the harmonic adsorption recuperative power (HARP) system concept. The HARP concept introduces PNNL's patented [2] multibed heat engine architecture directly into the power generation cycle. The working fluid is never physically condensed in this system. However, by using a sorbent with a very strong chemical affinity for the working fluid, near liquid phase densities are achieved in the adsorption beds. By avoiding the need for condensation, this system can also impose a larger pressure drop across the engine and generate more power. The impact of this enhanced pressure drop can be quantified with a simple energy balance calculation. Power generation (P) is given by:

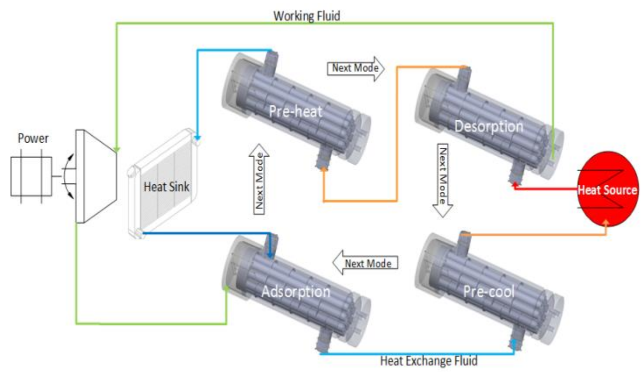

Figure 2. Schematic of HARP System Concept.

$$P = \eta_e \dot{m}_r (h_r^1 - h_r^o) \quad (1)$$

where η_e is the efficiency of the expander (engine), $\dot{m}_r$ is the working fluid mass flow rate, h_r^1 and h_r^o are the outlet and inlet enthalpy across the engine, respectively. Heat flows across an adsorption bed are given by:

$$(1-\eta_h)\left[\dot{m}_r \Delta H_a t_c + (m_{Al} c_p^{Al} + m_s c_p^s + m_v c_p^v)(T_h - T_L)\right] = \dot{m}_w (h_w^1 - h_w^o) \quad (2)$$

where η_h is the recuperation efficiency between beds, ΔH_a is the heat of adsorption, t_c is the bed cycle time, m_{Al}, m_s, and m_v are the masses of aluminum, sorbent, and refrigerant vapor in the adsorption bed, c_p^i are the corresponding heat capacities, and T_h and T_L are the high and low temperatures of the bed during a cycle. The right hand side of Equation (2) represents the balancing heat rejection to the environment through either cooling water or an air-cooled heat exchanger. The sorbent mass required can be estimated from:

$$m_s = \frac{\dot{m}_r}{f_r} t_c \quad (3)$$

where f_r is the net change in refrigerant loading across the cycle and t_c is the cycle time . Using the assumed parameters in Table 1, the HARP system power output is predicted to increase to 7.4 kW (or 42%) with the identical R134a flow rate of 0.65 kg/s and average output condition from the ORC engine of 30°C and 7.5 bar. Moreover, the heat dissipation required drops from 120 kW to 96 kW. This calculation assumes an unchanged state point input to the engine of 86°C and 30 bar. However, it should be possible to increase the power output further by using the adsorption modules to increase the input temperature and pressure above what is economic via a standard evaporator. This is because heat is transferred to the refrigerant through highly efficient heat exchanger modules and concentrated refrigerant (very near liquid density) adsorbed in the pore structure of the sorbent material(s) filling the modules. Heat can, therefore, be added efficiently to the refrigerant until a desired pressure and temperature are reached, which can exceed the state point conditions of the standard design. Both of these factors provide opportunity for significantly higher power output from the HARP system with the equivalent heat input and lower heat dissipation required to the environment.

Table 1. HARP System Example Heat Balance Parameters

Parameter	Value	Units
η_e	0.9	
T_h	140	°C
T_L	30	°C
h_r^o	427	kJ/kg
h_r^1	415	kJ/kg
$\dot{m}_r$	0.65	kg/s
t_c	60	s
f_r	130%	wt%
m_s	30.1	kg
m_v	0.96	kg
ΔH_a	350	kJ/kg
m_{Al}	24.1	kg
c_p^v	1.1	kJ/kg·K
c_p^s	0.9	kJ/kg·K
c_p^{Al}	0.9	kJ/kg·K
η_h	0.7	

Achieving the power increase estimates with this system hinges on having a high performance sorbent material that allows cycle times and refrigerant loadings consistent with the t_c and f_r values shown in Table 1. Fortunately at PNNL, we have been investigating high-capacity sorbents for fluorocarbon working fluids as part of a several R&D efforts on nanofluids [3]. **Error! Reference source not found.** shows adsorption isotherms for R134a with several sorbents discovered through this work. The highest capacity sorbent's (COF-4) refrigerant uptake is nearly 200 wt% as the relative saturation vapor pressure (P/P_o) approaches one, which is the expected condition for the output from the engine (input to the adsorption bed). Assuming a net working capacity of 130 wt% is achieved in a cycle, only about 30 kg of sorbent occupying 60L of space would be needed for the HARP system. Unfortunately, manufacturing cost for this sorbent is estimated at over $5000/kg, obviously prohibitively expensive for this application. Although we have evaluated many other fluorophilic sorbents [4], up until recently none have the performance of COF-4. A breakthrough occurred very recently where we have discovered a metal organic framework (MOF) sorbent that achieves the capacity of COF-4 at 100X cost reduction. Although we cannot reveal the composition of this sorbent in this paper, we can illustrate performance tests with it. Although we cannot reveal the composition of this sorbent in this paper, we can illustrate performance tests with it.

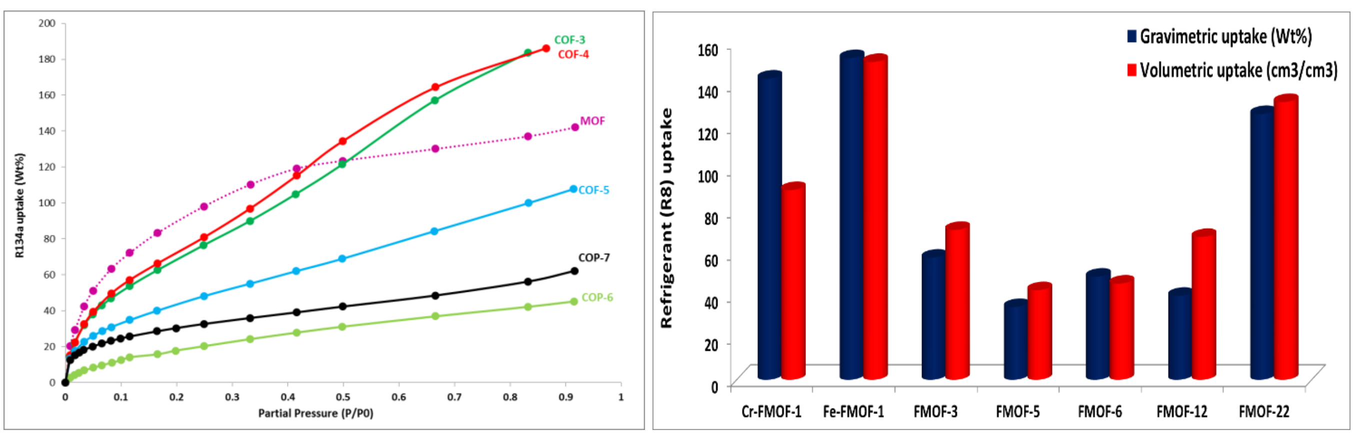

Figure 3. Adsorption isotherm for R134a refrigerant and several sorbents (left) and volumetric gravimetric loading of several flourophilic MOFs(right)

3. Design

The thermal compressor is at the heart of the HARP system. Driven by heat, it provides the motive force to transport the working fluid through the expansion engine, or a cooling cycle. We have developed numerous concepts for the internal structures of thermal compressors used in adsorption systems. Some of these concepts have been built and are currently being tested in our Thermal Compressor Test Facility (TCTF). Critical to power generation applications is a design that can withstand high pressures and a very large number of thermal cycles without failure.

After a concept has been designed and its performance simulated, and it has been determined that the concept will perform well from a heat and mass transfer perspective, it is tested in the TCTF. The adsorption module is charged with sorbent and refrigerant and cycled. Key performance criteria such as cycle time, compression ratio, and heat exchange fluid flow rates can be adjusted on-the-fly to optimize the operating parameters. Thousands of cycles must be run to understand if there is any degradation in performance or structural integrity of the design.

Any concepts that survive testing are beholden to manufacturability. Cost in manufacturing is the bottleneck that ultimately provides the decision for mass-producing one concept versus another. PNNL considers all methods of manufacturing including casting, brazing, extruding and additive manufacturing (printing) of parts. A combination of all or some of these methods will lead to the most cost effective and efficient thermal compressor.

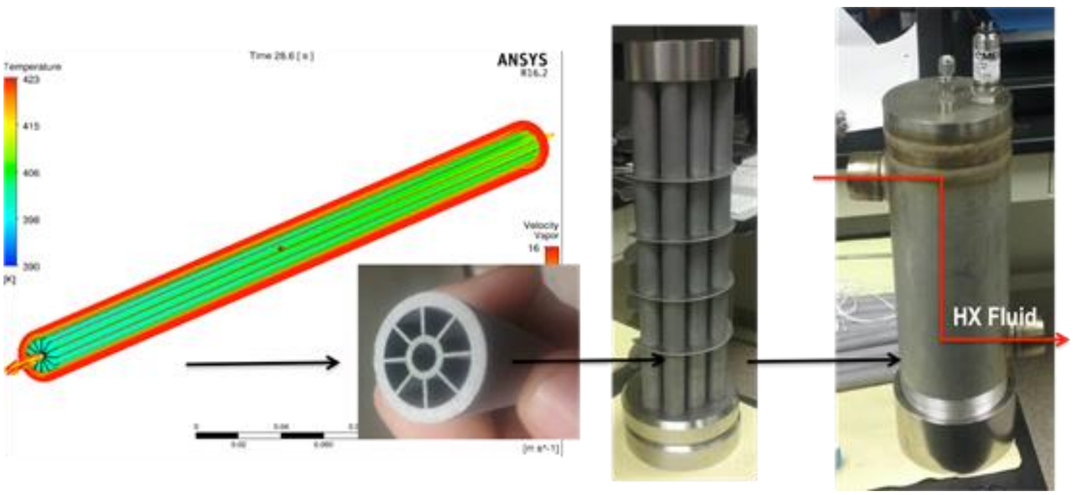

Figure 4. Rapid Prototype Development Process: Shell/Tube Concept

Figure 4 illustrates an example of this rapid prototype development process for a tube-in-shell concept. In this concept, each tube is 3D-printed using aluminum. The tubes are then fitted with baffels and enclosed in a stainless steel shell. The tube geometry is unique and has never been considered for these types of systems. The inner tube is a porous structure that allows refrigerant to pass into and out of the sorbent (sorbent shown in blue/green on left CFD image). The fins enhance the heat transfer from the heat exchange fluid that flows around the outer tube. This concept has several adavantages including ease of manufacturing and assembling. The 12-tube test section shown is continously underwent cycle tests at the TCTF.

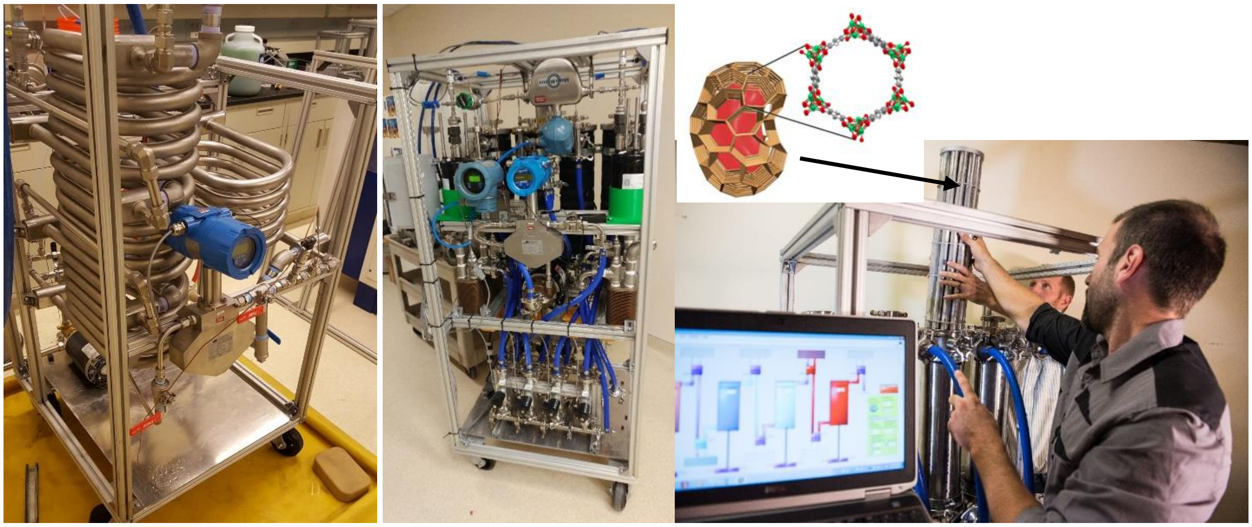

Figure 5. Image of Standard ORC(left), HARP(middle), Heat/Mass Exchanger Assembly(right)

After initial cycle testing at the TCTF, a four-bed system was designed around a tube-in-shell concept illustrated in Figure 4. This system was constructed in our advanced energy systems lab (ARES). The HARP system shown at the center of Figure 5 is a fully autonomous system with user inputs capable of providing thermally driven compression for cooling and power systems.

1. Results

Data presented here shows the parameters required for a thermal compressor design. The most critical parameters are volumetric refrigerant loading and cycle time. It is important to note that the cycle time is directly proportional to the size of the thermal compressor. Additionally, refrigerant loading kinetics for a given sorbent play a major role in that time.

Figure 6 shows the pressure and temperature swing results with two different sorbents packed into a single copper tube. KBB is a commercially available activated carbon and is compared with the MOF sorbent. The data from Figure 6 shows that the MOF generates 500 psia (34 bar) 30% faster than the KBB. In addition, the sorbent loads over 30% more refrigerant per unit volume than KBB. Because compression speed and capacity are additive effects, selecting the MOF sorbent would result in a 60% smaller thermal compressor delivering the same power output.

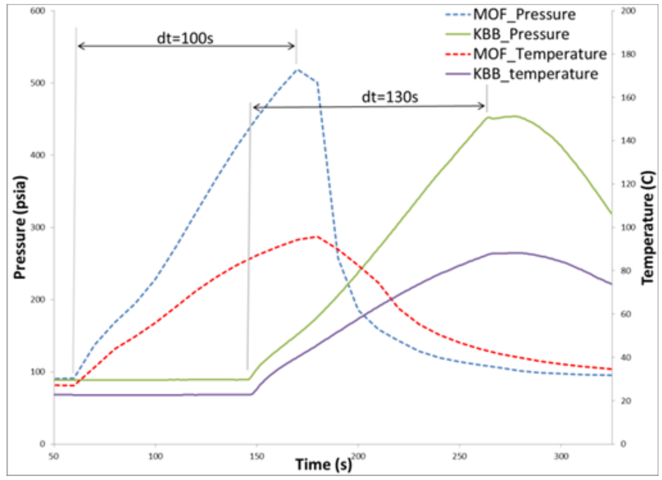

Figure 6. MOF and Activated Carbon (KBB) Cycles with R134a in Finned Tube

Figure 7 shows several automated cycles completed in the TCTF using KBB and R134a loaded into the shell-tube heat exchanger design. The cycle time was fixed at 90 s to achieve a compression ratio of 30:1. Critical to generating sufficient work from the fluid through the expander is a high inlet enthalpy and low discharge enthalpy. These data show that the R134a pressure reaches 30 bar in less than 100 s and maintains a temperature of 140ºC during desorption. During adsorption the pressure drops to 1 bar and maintains a temperature of 20ºC. The mass loading fraction during adsorption and desorption was found to be just over 1.3 g/g as determined from mass flow data. As impressive as these numbers are, we expect the cycle time will be reduced by 30% using the MOF while delivering 30% more refrigerant flow. Testing with the FMOF is currently in progress. Due to the multibed configuration used in a complete HARP system, the time required to reach 30 bar is compensated by another bed completing its desorption cycle. With appropriate valve control logic and timing, constant working fluid flow has been achieved. Absolute pressures at the engine inlet and outlet are allowed to vary during the cycle while maintaining an approximately constant or nearly constant pressure differential across the engine.

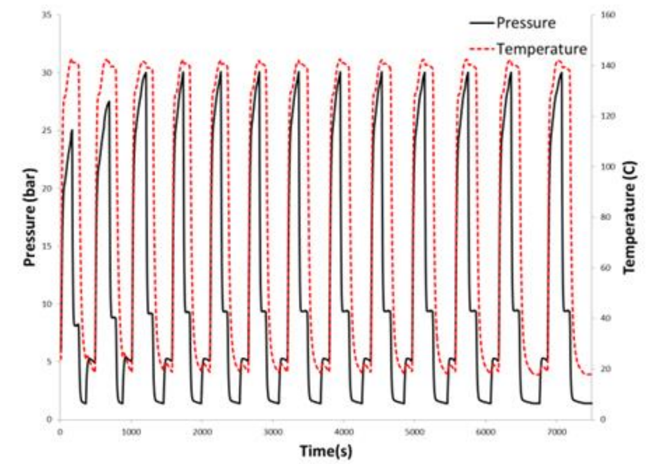

Figure 7. Thermal cycles of KBB/R134a in the shell-tube concept tested in PNNL's TCTF

Although testing to date has focused on R134a, we have collected adsorption data on many other refrigerants, including the new class of low global warming potential refrigerants like R1234yf and R1233ze. As the adsorption process involves relatively weak van der Waals bonds, we have observed no degradation of any refrigerant examined so far, even after hundreds or thousands of cycles.

The results from the 4-bed system using KBB and R134a are shown in Figure 8 and Figure 9. At relatively modest maximum pressures of 20 bar as shown on the left chart of Figure 8, average working fluid mass flow rates of 600 g/min were achieved. More notable is the operation of the system at a heat rejection of 30 ºC, a condenser temperature for which a typical ORC using r134a would nearly shutdown. This is one of the major benefits of the HARP cycle. Tests are currently underway to swing the pressure of the compressor to 30 bar, yielding expected power outputs of roughly 1 kW for this system.

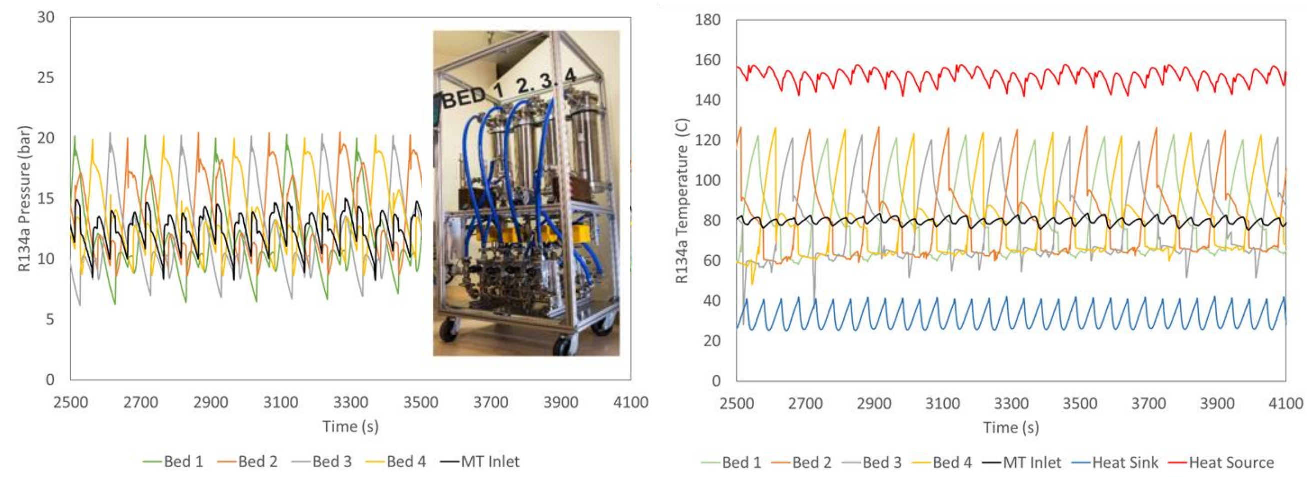

Figure 8. Thermal cycles of 4-bed KBB/R134a in the shell-tube concept tested in PNNL's ARES lab. MT is the microturbine.

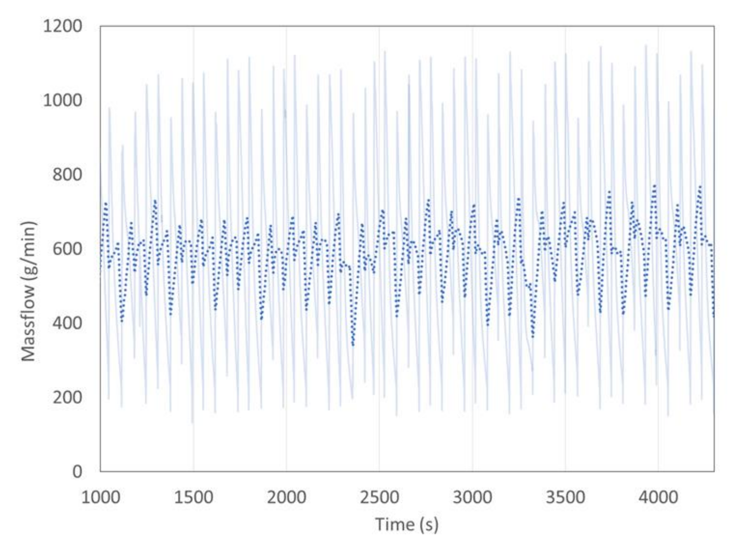

Figure 9. Continuous average mass-flow of 600 g/min using 4-bed system

RadMax has designed a rotary sliding vane expander for testing with our thermal compressor, as shown in Figure 10. The sliding vane expander operates by forming individual chambers between each pair of two vanes on both side of the rotor.The chamber

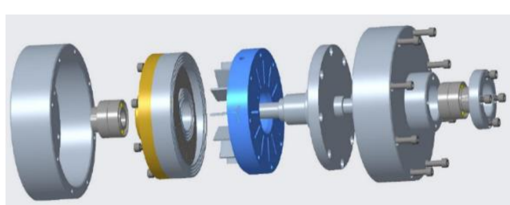

Figure 10. Radmax rotary sliding vane expander

volume between the vanes changes as the vane follows along a cam profile that results in alternately compressing and expanding fluids at both cam locations. Attributes to the Radmax deisgn include positive displacement, low speed (1800 RPM), operation at low pressure/flow-rate compared to existing turbomachinery. We will be generating electricity with the Radmax unit and measuring power output using a load-bank.

The above geometry will yield an expander with a letdown ratio of 7.5. With R134a as the fluid, a flowrate of 766 grams per minute, it is predicted to produce 0.64 kW of power with an inlet pressure of 20 bar and 120^0 C for the inlet temperature. The aforementioned performance predictions for this expander are detailed in Figure 11. We expect to push this boundary to 30 bar, generating upto 1 kWe-. The predicted performance is based on 85% isentropic efficiency.

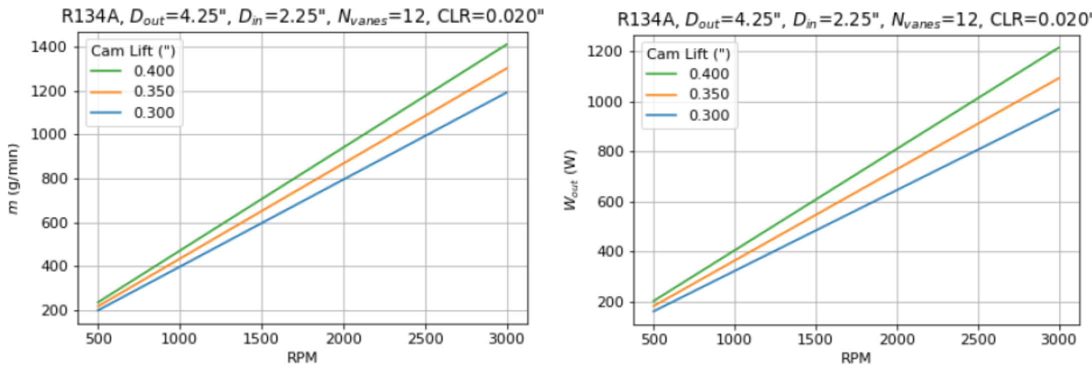

Figure 11. Radmax rotary sliding vane expander performance

Table 2. Cost Analysis Parameters and LCOE Estimates for HARP System.

SYSTEM CONFIGURATION	UNIT	HARP
Number of expanders	Units	4
Heat consumption	kW	273
Net electric power	kW	58
Annual operating hours	hours	8,300
Net electricity production	kWh	481,400

O&M ITEMS	UNIT	HARP
Period of depreciation	Years	10
Annual insurance cost	$	1,059
Annual service cost	$	5,000
Straight Line Depreciation*	$	(2,433)

CAPITAL COST ITEMS	1st Gen	Production
CraftEngine™ System (incl. PowerPack Converter)	48,000	48,000
Thermal Compressor	191,340	55,615
Site Installation	19,000	19,000
Total profit (20% OH and G&A;20%EBIT)	49,046	49,046
Net investment cost	**307,386**	**171,661**

BUDGET PARAMETERS	UNIT	LCOE 1st Gen	LCOE Production
Production cost per kWh	$/kWh	**0.076**	**0.048**
Investment cost per kW	$/kW	5300	2960

*Not included in LCOE estimates

2. Cost Analysis

The cost of manufacturing the HARP system was estimated by developing a detailed bill of materials and obtaining quotes from suppliers for each component in the system. A similar approach was used to estimate cost of manufacturing the sorbent material that includes raw materials costs for the chemical precursors, necessary solvents, capital and operating cost estimates for the production system, and shipping and margin costs to derive a production cost estimate for the sorbent. By rolling up both component and sorbent costs, a total system cost can thus be developed.

Table 1 provides an example of the bill of materials developed for a 40 kW nominal standard ORC system that is upgraded with the HARP thermal compressor and so produces a nominal power output of 58 kW. Costs of the raw materials including MOF sorbent was estimated based on 1,000 unit sales of the systems. The key metric in this table is the estimated total LCOE or levelized cost of electricity produced by the system. Significantly, the LCOE of even the first of these units produced at PNNL resulted in an attractive LCOE estimate just under $0.08/kWh. LCOE estimates drop to under $0.05/kWh with 1000 unit production. These numbers provide sufficient margin to produce a very attractive rate of return for HARP systems deployed in the U.S. and of course even better in remote locations such as Alaska and Hawaii, the EU, Australia, etc where electric power prices are considerably higher.

3. Conclusion

A new power cycle has been presented that uses a multibed recuperative thermal compressor in place of standard ORC components. A heat balance calculation suggests that at least 40% more power can be generated using the HARP technology. Thermal compressor testing has proven that the necessary working fluid flows and compression power is produced with a suitable heat exchanger design. Cycle performance testing is continuing with several heat exchanger designs to obtain reliability data that can feed an overall techno-economic analysis of the system. Present estimates show the HARP system can generate power with a 100°C to 150°C heat source at <$0.10/kWh – a true breakthrough in price/performance for this class of system.

References

[1] Quoilin S, Orosz M, Hemond H, Lemort V. Performance and design optimization of a low-cost solar organic Rankine cycle for remote power generation. Solar Energy. 2011;85:955-66.

[2] Wegeng RS, Rassat SD, Stenkamp VS, TeGrotenhuis WE, Matson DW, Drost MK, et al. Apparatus for thermal swing adsorption and thermally-enhanced pressure swing adsorption. In: Office USPT, editor. United States: Battelle Memorial Institute, Richland, Washington; 2005.

[3] McGrail BP, Thallapally PK, Blanchard J, Nune SK, Jenks JJ, Dang LX. Metal Organic Heat Carrier Nanofluids. Nano Energy. 2013;2:845–55.

[4] Motkuri RK, Annapureddy HVR, Vijaykumar M, Schaef HT, Martin PF, McGrail BP, et al. Fluorocarbon adsorption in hierarchical porous frameworks. Nat Commun. 2014;5.